Electrical-conduction mechanisms in polymer–copper-particle composites. II. (1/f)-noise measurements in the percolation limit

C. Pierre and R. Deltour
Physique des Solides, CP233, Université Libre de Bruxelles, boulevard du Triomphe, B-1050 Bruxelles, Belgium

J. Van Bentum and J. A. A. J. Perenboom
Research Institute for Materials and High-Field Magnet Laboratory, University of Nijmegen, Toernooiveld, NL-6525 ED Nijmegen, The Netherlands

R. Rammal
Centre de Recherche sur les Très Basses Températures, Centre National de la Recherche Scientifique, Boîte Postale 166X, F-38042 Grenoble, France
(Received 5 January 1990)

We have investigated the mechanisms of electrical conduction of polymer–copper-particle composites in the low-particle-concentration limit (dilute limit) by electrical-noise measurements. The $1/f$ flicker noise, observed close to the percolation threshold, has been studied as a function of the current through the sample, frequency (10^{-2}–10^{4} Hz), and resistance (10^{1}–10^{9} Ω). In this paper we relate the total resistance noise measured on the samples to the local noise due to the different contacts between the particles. The resistance and noise power of the inhomogeneous medium is modeled by an extended effective-medium theory that includes a transition between two different conduction mechanisms near the percolation threshold. This model gives support to our hypothesis that the noise is produced by small electrical contacts between the particles, as well as the node-link picture introduced to characterize the conductive backbone preexisting at the percolation transition in the continuous percolation models.

I. 1/f NOISE IN COMPOSITE SYSTEMS

Although many experiments have recently shown that impurities can give rise to $1/f$ electric field fluctuations in metals,[1–5] there is at present no general microscopic theory for the electrical noise in various solid-state physical systems.[6–9] This noise, different from the thermal noise that, at low frequency, only depends on resistance and temperature, is also sensitive to the dc current passing through the sample and the frequency. In a disordered system, as in the case of the conducting polymer-particle systems we are considering, the total resistance R is a moment of order 2 of the currents i_α flowing through different conduction paths α, each characterized by the value of its resistance r_α,[10]

$$R=\frac{\sum_\alpha i_\alpha^2 r_\alpha}{I^2}\ , \tag{1}$$

where I is the total current through the sample. In contrast, the resistance fluctuations are moment of order 4 of the current i_α,

$$\langle \delta R^2\rangle=\frac{\sum_\alpha i_\alpha^4 \langle \delta r_\alpha^2\rangle}{I^4}\ . \tag{2}$$

The noise power is therefore a very sensitive probe of inhomogeneities in the conductor.[11–17] It will be shown that, although the noise power and the electrical resistance of the samples are rapidly diverging when the percolation limit is approached, study of the noise power at the percolation threshold versus the electrical resistance of the same samples allow us to get rid of the unavoidable local inhomogeneities in particle distribution which otherwise could only be eliminated by a prohibitive number of experiments.

In 1958, Holm[18] published his trend-setting work in which he related the total $1/f$-noise power in carbon-membrane microphones to the supposedly uncorrelated noise at the particle interfaces. Later, Williams and Burdett[19] and Celasco and co-workers[20] studied the noise spectra of evaporated thin gold films. Chen and Chou[21] have more recently investigated systems very similar to the ones discussed in this paper, carbon-black-loaded resin, and have observed a divergence of the noise power as the particle concentration approaches the percolation limit at p_c.

$$\mathcal{S}_R=\frac{\langle \delta R^2\rangle}{R^2}\approx(p-p_c)^{-K}\ , \tag{3}$$

with $K=5$.

By substituting the concentration dependence of R near the percolation threshold, this can also be rewritten as $\mathcal{S}_R\sim R^{\omega}$, where, in this case,[21] $\omega=1.7$. The noise is attributed to fluctuations of the number of charge carriers along the infinite conduction paths through the clus-

 ©1990 The American Physical Society

ters preexisting at the percolation threshold. Garfunkel and Weisman[22] have studied the noise power as a function of resistance in randomly perforated Al, In, and Cr foils. They have observed ω values between 5.4 and 6.1 for a rather limited range of resistance values, and these high values can only be explained in a continuous percolation scheme. Koch *et al.*[23] have studied the $1/f$ noise as a function of R in evaporated gold films and found ω values close to 2, the value found earlier by Williams and Burdett.[19] These authors observed a variation of the noise power with temperature and with the concentration of clusters close to the percolation threshold, and they attributed this variation to the transition from a metallic-conduction mechanism for the noise to a tunnel mechanism closer to the percolation threshold. Mantese, Webb and Curtin[24,25] have given a quantitative interpretation of their noise measurements in Al_2O_3-Pt cermets in terms of the two-component effective-medium theory developed by Rammal[26] for weakly disordered media. They have found that the noise power, which increases with resistance at the percolation threshold, saturates for high values of the sample resistance. Both the noise power and the resistivity show a change of dependence with temperature at the percolation transition, which they attribute to the same two mechanisms: a transition from metalliclike to tunneling through oxide barriers for the more resistive samples. Finally, Octavio *et al.*[27] have also obtained the values $\omega = 1.2$ and 2.7 for two different percolating systems at liquid-nitrogen temperature.

II. $1/f$ ELECTRICAL NOISE DUE TO CONTACT RESISTANCES

For small volume conducting systems, Hooge has formulated an empirical law to describe the electrical noise S_v as a function of various parameters:[6]

$$\mathcal{S}_v(f) = \langle \delta V^2 \rangle = \alpha \frac{V_{dc}^{2+\epsilon} \Delta f}{N f^{\gamma}} , \qquad (4)$$

with $\epsilon \approx 0$, $\gamma \approx 1$, and α a dimensionless constant of $\approx 2\times 10^{-3}$. In Eq. (4) f is the frequency, V_{dc} is the dc voltage along the sample, N is the total number of charge carriers, and Δf denotes the bandwidth of the measuring instrument. From this relation, widely discussed in the literature, S_v is inversely proportional to the total number N of charge carriers in the sample: $N = nV$ where n is the charge carrier density and V the volume of the sample. This relation $S_v \sim N^{-1}$ implies a bulk source for the noise process and can be viewed, because of Ohm's law, as the signature of fluctuations of the charge-carrier mobility. This dependence of S_v versus N^{-1} is controversial and is not the purpose of our discussion here. Let us just mention that in some semiconductors, for example, the noise power depends on the number of surface states, and Eq. (4) is no longer justified.

The most significant part of Eq. (4) is probably the square-law dependence on the voltage across the sample. Indeed, such a behavior is quite universally obeyed, and this indicates that this $1/f$ noise stems from resistance fluctuations, independent of the dc current:

$$\langle \delta V^2 \rangle = I_{dc}^2 \langle \delta R^2 \rangle . \qquad (5)$$

In this respect, the current acts as a very useful amplifier, eventually allowing one to extract this $1/f$ noise from the thermodynamic noise.

In the study presented in the preceding paper,[28] we have found that the resistance in the high-concentration metal-polymer composites is due to electrical transport across the microcontacts between the metallic particles. We expect, therefore, that the noise observed in our samples near the percolation transition is related to the noise produced by these microbridges. In order to go further in this direction, let us recall the basic features of the $1/f$ noise due to contact resistances.

(a) For two metallic spheres in contact with a radial distribution of current lines, one finds that the noise power varies as the third power of the contact resistance when the mean free path l is much smaller than the contact radius a. This conduction regime is known as the Maxwell regime, and

$$\mathcal{S}_r \sim C_1(f) r^3 \quad \text{with } r = \rho / 2a . \qquad (6)$$

Here, $C_1(f) = \alpha\rho^2 / 20\pi^3 b^5 n f$, $b = 2a/\pi$, and ρ denotes the electrical resistivity. This law—$\mathcal{S}_r \sim r^3$—is very well established both theoretically and experimentally.[29-31]

(b) In the opposite limit of a contact in the ballistic regime $l \gg a$ (the so-called Sharvin regime), Akimenko, Verkin, and Yanson[29] have found that the noise power is inversely proportional to the contact volume, $\mathcal{S}_r \sim 1/a^3$, still in agreement with Eq. (4). Using Sharvin's formula for the contact resistance[28]

$$r = \frac{4}{3\pi} \frac{\rho l}{a^2} , \qquad (7)$$

one gets a $\frac{3}{2}$-law dependence of the noise power on contact resistance,

$$\mathcal{S}_r \approx C_2(f) r^{3/2} . \qquad (8)$$

(c) Finally, for a noisy conducting oxide contact, such as the cuprous oxide Cu_2O, one finds[30]

$$\langle \delta r^2 \rangle = \langle \delta r_{\text{oxide}}^2 \rangle + \langle \delta r_{\text{contact}}^2 \rangle , \qquad (9)$$

and if the oxide film dominates $\langle \delta r_{\text{oxide}}^2 \rangle \gg \langle \delta r_{\text{contact}}^2 \rangle$, the functional dependence on r of the noise power becomes

$$\mathcal{S}_r = \frac{\alpha}{N_{ox} f} = C_3(f) r^1 \qquad (10)$$

and

$$r = \frac{\rho_{ox} t}{\pi a^2} , \qquad (11)$$

where t denotes the oxide layer thickness and ρ_{ox} its resistivity. In Eq. (10) the noise power is inversely proportional to the number of charge carriers in the oxide layer, N_{ox}.

III. $1/f$ NOISE IN A RANDOM RESISTOR NETWORK

A. Perfect resistor network

Let us first consider an ideal hypercubic lattice of identical resistors ($r = r_i$), each having a noise power

$$\mathcal{S}_r = C r^{\omega} , \tag{12}$$

where ω is a given exponent. If one assumes that such a network is made of contact resistors between metallic spheres, then ω is given by 3, $\frac{3}{2}$, or 1, as discussed above for the three different types of contacts, C being a constant equal to C_1, C_2, or C_3.

If R is the total resistance and $\mathcal{S}_R$ the total noise power of this network, then using the composition rules of noisy resistors (in series or parallel),[10] one finds

$$\mathcal{S}_R = C R^{\omega} L^{\omega(d-2)-d} \tag{13}$$

and

$$R = r / L^{d-2} . \tag{14}$$

Here, L^d is the total number of elementary resistors, d being the dimensionality of the lattice. Two remarks are in order regarding Eqs. (13) and (14). One notices first that the functional relation $\mathcal{S}_r \sim r^{\omega}$ is preserved from the elementary resistor to the whole network. The second remark is the size dependence $\mathcal{S}_R \sim L^{-d}\mathcal{S}_r$, which agrees with Eq. (4). For instance, in two dimensions ($d=2$), Eq. (13) gives back the well-known result that a square lattice of noisy resistors gives a total noise power which is $1/L^2$ times smaller than that of an equivalent resistor, $R = r$, carrying the same total current.

It is important to notice that the above two properties are somehow specific to homogeneous systems (i.e., regular networks). The purpose of the following subsections is to study those properties which survive in a disordered network.

B. Effective-medium theory

Disorder can be modeled in the perfect network just discussed by specifying the probability distribution $p(g_i, \mathcal{S}_i)$ that a bond i has a conductance g_i and noise power $\mathcal{S}_i$. This is a simple model for our composite system viewed as a resistor network made of contact resistances. An efficient method to describe such a system is the so-called effective-medium theory. The basic idea is to replace the disordered network by a perfect one made of identical elements g_m and $\mathcal{S}_m$. The self-consistent effective-medium equations for g_m and $\mathcal{S}_m$ are[26]

$$\langle g^{-1} \rangle = \int dg_i d\mathcal{S}_i p(g_i, \mathcal{S}_i) \frac{1}{g_i + \alpha g_m} = \frac{1}{(1+\alpha) g_m} , \tag{15}$$

$$\langle \mathcal{S} \rangle = \int dg_i \, d\mathcal{S}_i \, p(g_i, \mathcal{S}_i) \frac{g_i^2 \mathcal{S}_i + \alpha^2 \beta g_m^2 \mathcal{S}_m}{(g_i + \alpha g_m)^2} = \frac{1+\alpha^2\beta}{(1+\alpha)^2} \mathcal{S}_m . \tag{16}$$

Here, g_m and $\mathcal{S}_m$ represent the unknown values of the conductance and the noise power of the effective lattice. Furthermore $\alpha = z/2 - 1 = 1/\beta$, where z is the coordination number of the lattice. Therefore, Eq. (16) can also be written $\langle \mathcal{S} \rangle = \mathcal{S}_m / (1+\alpha)$.

Let us illustrate the general equations (15) and (16) in some particular cases where the probability distribution is as simple as possible.

(a) *Dilution disorder:* This case corresponds to a disorder introduced by removing some resistors from the otherwise perfect network. Let p denote the probability of finding a resistor (conductance g_0 and noise power $\mathcal{S}_0$) at bond i. This leads to the following expression for $p(g_i, \mathcal{S}_i)$:

$$p(g_i, \mathcal{S}_i) = p\delta(g_i - g_0)\delta(\mathcal{S}_i - \mathcal{S}_0) + (1-p)\delta(g_i)\delta(\mathcal{S}_i) . \tag{17}$$

This discrete distribution for $(g_i, \mathcal{S}_i)$ allows for a simple solution of Eqs. (15) and (16). Indeed, we find the known results[26]

$$\frac{g_m}{g_0} = \frac{z}{z-2}(p - p_c)^1, \quad \frac{\mathcal{S}_m}{\mathcal{S}_0} = \frac{z-2}{z}(p - p_c)^{-1} \text{ at } p > p_c , \tag{18}$$

$$\frac{g_m}{g_0} = \frac{\mathcal{S}_m}{\mathcal{S}_0} = 0 \quad \text{at } p < p_c . \tag{19}$$

The percolation threshold $p_c = 2/z$ corresponds to the effective-medium value for the percolation transition between a conductor ($p \ge p_c$) and an insulator ($p \le p_c$).

Notice that when $p - p_c$ is eliminated between g_m and $\mathcal{S}_m$, one obtains a very simple result:

$$\mathcal{S}_m = \frac{\mathcal{S}_0}{R_0} R_m . \tag{20}$$

Equation (20) is actually a particular case of a more general result (see below) relating $\mathcal{S}_m$ to R_m. Let us recall that the effective-medium results are qualitatively good, but provide a poor picture of the critical fluctuation regime near p_c. Indeed, Eq. (18) provides good quantitative results far away from p_c, i.e., at $p \le 1$ or in situations where g_i's and $\mathcal{S}_i$'s remain finite (see below, the two-component model).

(b) *Continuous distribution:* Let us now consider a more realistic distribution, $p(g_i, \mathcal{S}_i)$,

$$p(g_i, \mathcal{S}_i) = p h(g_i, \mathcal{S}_i) + (1-p)\delta(g_i)\delta(\mathcal{S}_i) . \tag{21}$$

For the sake of simplicity, we shall consider the case where $\mathcal{S}_i$ is determined by g_i. This means that g_i is the only random variable, and $\mathcal{S}_i$ is given by a function of g_i. Furthermore, we assume

$$h(g_i \le 1) = A g_i^{\mu}, \quad h(g_i \ge 1) = 0 . \tag{22}$$

The normalization constant A and the exponent μ are related by the norm condition

$$A \int_0^1 g^{-\mu} dg = 1, \quad 0 < \mu < 1 . \tag{23}$$

Using Eq. (15), we get back the known result for g_m:[32]

$$g_m \approx (p-p_c)^{1+\delta} , \tag{24}$$

with $\delta=\mu/(1-\mu)$. This shows, in particular, that even the effective-medium theory will give critical exponents which depend on the distribution of conductances.

Equation (16) allows for the determination of $\mathcal{S}_m$ when $\mathcal{S}_i$ versus g_i is known. Instead, without going into such details, let us relate $\mathcal{S}_m$ to g_m in the most general case. For this, we proceed by eliminating the probability p from Eqs. (15) and (16), after using Eq. (21). This leads to the general result

$$g_m \mathcal{S}_m = \frac{\int dg_i d\mathcal{S}_i h(g_i,\mathcal{S}_i) \dfrac{g_i^2 \mathcal{S}_i}{(g_i+\alpha g_m)^2}}{\int dg_i d\mathcal{S}_i h(g_i,\mathcal{S}_i) \dfrac{g_i}{(g_i+\alpha g_m)^2}} = \frac{\left\langle \dfrac{g_i^2 \mathcal{S}_i}{(g_i+\alpha g_m)^2} \right\rangle}{\left\langle \dfrac{g_i}{(g_i+\alpha g_m)^2} \right\rangle} . \tag{25}$$

As a matter of illustration, let us assume that there is a relation between the conductance g_i and its noise power $\mathcal{S}_i$:

$$\mathcal{S}_i = C g_i^{-\omega} . \tag{26}$$

Using Eq. (25), it is easy to derive the following result:

$$\mathcal{S}_m = B R_m^{\omega} = B g_m^{-\omega} . \tag{27}$$

Here, B refers to a numerical constant which depends on the specific probability distribution $h(g_i)$, but is independent of g_m. For the particular case chosen, Eq. (21) the convergence conditions require $0<3-\omega-\mu<2$.

Equation (27) is expected to hold under more general conditions, providing a sufficiently regular distribution $h(g)$. This simply means that one gets the same functional dependence for $\mathcal{S}_m$ versus g_m and $\mathcal{S}_i$ versus g_i.

IV. MEASUREMENTS

A dc current, with a value between 10^{-10} and 10^{-3} A, derived from a low-noise Tadiran model TL2150 battery, is injected into the sample, prepared as described in Ref. 28. The voltage fluctuations were measured using a low-noise Princeton Applied Research model 113 preamplifier and spectrally analyzed in a high-speed Brüel and Kjaer model 2032 Fourier analyzer. The accumulated data were computer analyzed and averaged.

For the low-resistance values, $10^1 < R < 10^6$ Ω, we have taken the Fourier transform of the intercorrelation function of the amplified signals from the sample along two parallel channels. This allows one to reject noise components from the preamplification stage.

For the noise measurements on the highly resistive samples, $10^5 < R < 10^9$ Ω, when the power transfer is maximum a single amplifier detection scheme was preferred, and in this case we have measured the Fourier transform of the autocorrelation function.[33,34]

For each sample we measured noise-power–dc-current characteristics for at least four different values of the current through the sample in a bandwidth range 6.25×10^{-2}–50 Hz. For the highest current value (with the highest sample-noise–amplifier-noise ratio), we analyzed the noise spectrum from 10^{-2} to 10^4 Hz on the various bandwidth ranges of the instrument. At the lowest frequencies we accumulated at least 50 independent spectra for every resistance value, and at the highest

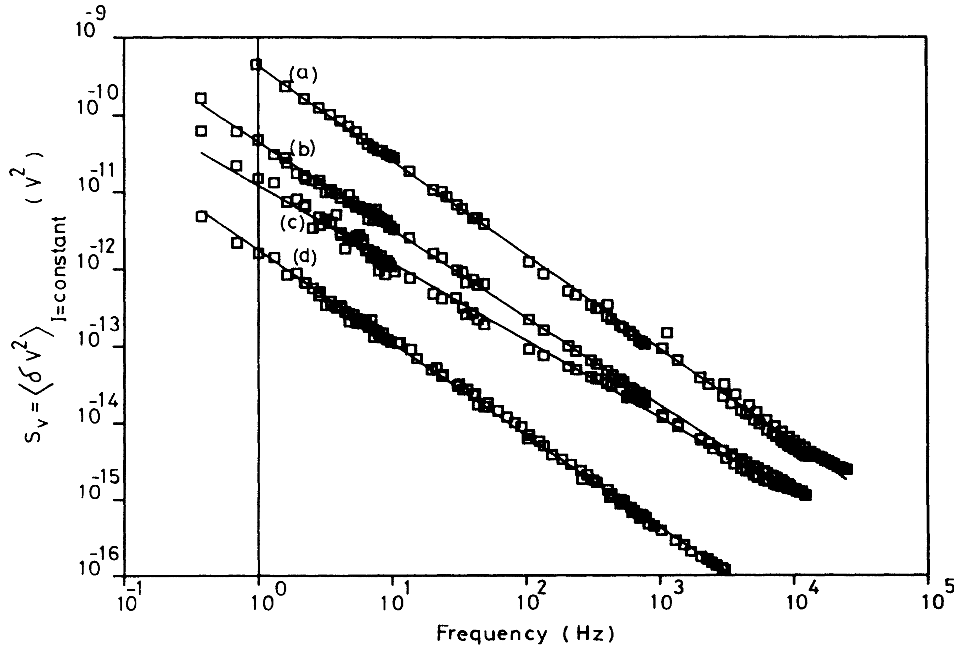

FIG. 1. Noise power $S_v = \langle \delta V^2 \rangle_{I=\text{const}}$ vs frequency f for several different values of the sample resistance R near the percolation threshold. (a) $\gamma=1.22$, $R=2.64\times10^4$ Ω, $P=3.0\times10^{-9}$ W; (b) $\gamma=1.14$, $R=1.42\times10^5$ Ω, $P=2.1\times10^{-10}$ W; (c) $\gamma=1.00$, $R=1.55\times10^7$ Ω, $P=1.7\times10^{-10}$ W; (d) $\gamma=1.2$, $R=1.2\times10^2$ Ω, $P=3.6\times10^{-5}$ W.

frequencies a few thousand have been averaged.

The curves presented in Fig. 1 represent typical noise-power, $S_v = \langle \delta V^2 \rangle$, versus frequency data for different sample resistance values near the percolation threshold. We have also indicated the intensity of the current through the sample, the total dissipated power, and the γ exponent of the frequency dependence: $S_v \sim f^{-\gamma}$.

We have observed γ-exponent values between 1.0 and 1.4 for all samples. For the high-resistance range ($R > 10^6$ Ω) we found that γ is always close to unity ($\gamma = 1.00 \pm 0.01$). No dependence whatsoever of γ on the electric power dissipated in the sample has been observed.

Figure 2 shows the characteristic dependence of the noise power at 1 Hz on the dc current through the sample for several different values of the resistance. For most of the samples a pure quadratic behavior can be observed ($S_v \sim I^\beta$, $\beta = 2.0 \pm 0.2$).

Some discrepancies occur for resistances close to and somewhat below 10^6 Ω, where nonlinearities of the noise power as a function of the current may appear. In that resistance range, β values as high as 10 could be observed at high current densities. The few measurements that did not show the quadratic dependence of the noise power on the dc current were rejected and have not been included in our analysis. For instance, Fig. 3 shows the anomalous behavior of a sample measured a few times in the "critical" region of sample resistance around 1 MΩ: the noise power seems to oscillate between two states. This effect, which was well reproducible in some samples is not due to a change of the resistance value.

Samples with resistance values between 10^3 and 10^6 Ω are very sensitive to the application of overly high electric fields: if one applies an increasing potential difference to the sample, at some critical field value (a few tenths of V/cm, the resistance suddenly drops to a lower value. It is interesting to note that a sample with original value R'' and particle concentration C'', whose resistance jumps to a lower value, R' ($R' < R''$), when applying an overly high electric field, gives a noise power similar to that of a sample with a different particle concentration C' ($C' > C''$) with this same total resistance R'.

With an overly large current through the sample it was possible to irreversibly return to a large resistance value. We attribute this latter effect to the vaporization of the small metallic microbridge forming the contact between the particles, and this process was even accompanied by small luminous flashes, which could be observed by the eye. Similar switching characteristics have been observed in other systems[35,36] and are discussed later.

Figure 4(a) summarizes the most important results of this experimental work, and shows the averaged value of the noise power, measured at a frequency of 1 Hz and normalized by the square of the dc current, as a function of the sample resistance; the data are presented on

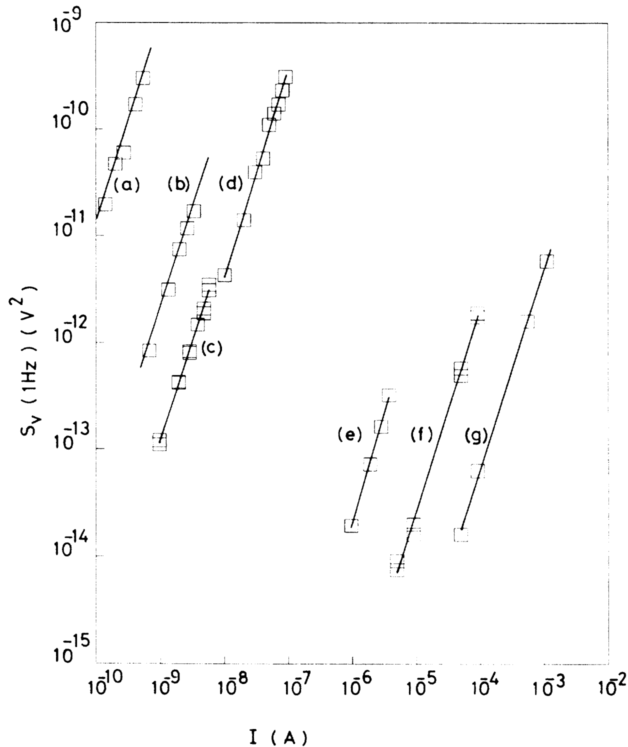

FIG. 2. Current dependence of the noise power S_v at 1 Hz for several different values of sample resistance near the percolation threshold. (a) $\beta=2.0$, $R=1.6\times10^8$ Ω; (b) $\beta=1.9$, $R=1.55\times10^7$ Ω; (c) $\beta=1.84$, $R=1.11\times10^6$ Ω; (d) $\beta=1.95$, $R=1.7\times10^5$ Ω; (e) $\beta=2.0$, $R=1.34\times10^3$ Ω; (f) $\beta=1.9$, $R=3.69\times10^2$ Ω; (g) $\beta=1.9$, $R=9.6\times10^1$ Ω.

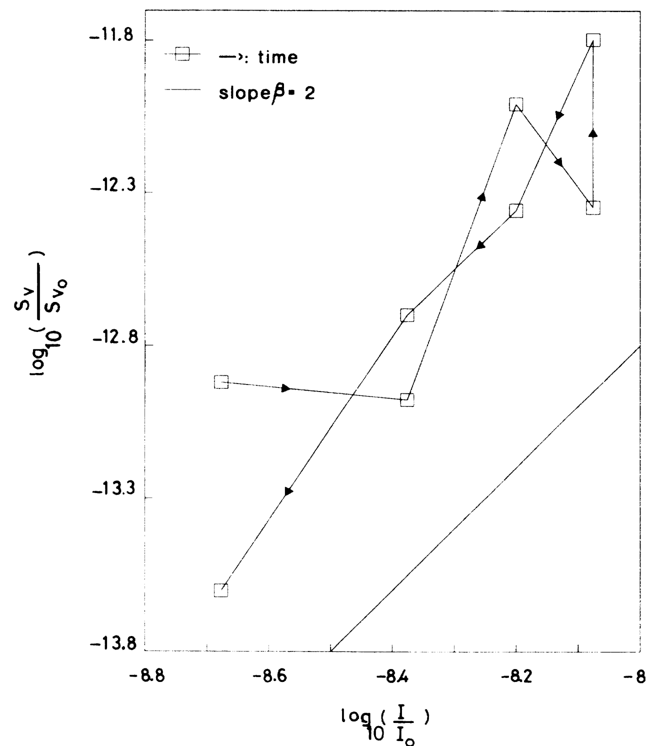

FIG. 3. Anomalous current dependence of the noise power observed in a sample with resistance in the "critical" region, $R=1.4\times10^5$ Ω. The arrows indicate the order in which measurements on this sample were taken; the solid line represents the slope $\beta=2$.

double-logarithmic scales to show clearly the R dependence: $\langle S_v/I^2\rangle \sim R^{\omega+2}$. Data for the two different types of copper powder (irregular and spherical) dispersed in polystyrene are presented. One can immediately notice the variation—by 18 orders of magnitude—of the noise power as a function of the sample resistance. Both types of powder show the same general behavior. The solid line is a fit to the theory to be discussed below.

Figure 4(b) shows the same results, but now normalized by the square of the voltage across the resistance. This curve will be more directly useful in the following discussion as the normalized noise power $\mathcal{S}_v = \langle \delta V^2\rangle / V^2$ is the dimensionless quantity generally discussed in the literature. One can distinctly observe in this double-logarithmic plot two linear regions with slightly different slopes, separated by two extrema.

We note that all data points in Fig. 4 are taken near the percolation threshold, with a surface concentration of copper particles between 0.7 and 0.9. In this regime the system consists of a single monolayer of conducting particles and can be described by a single two-dimensional percolation model.[28]

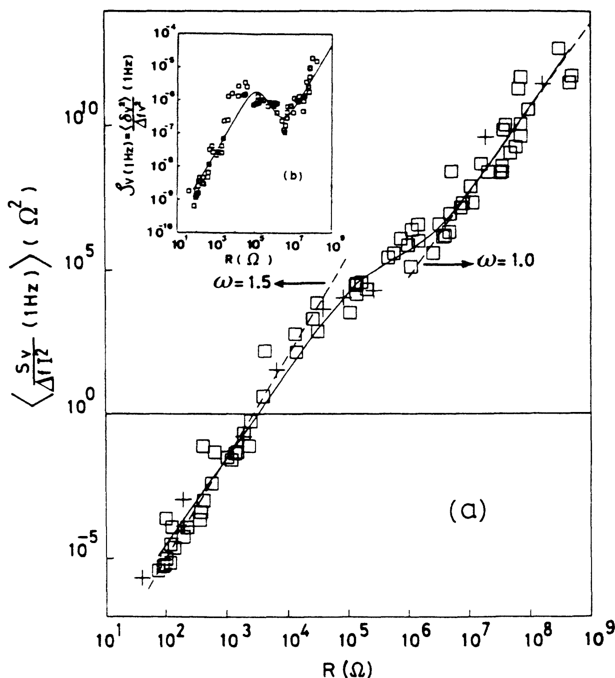

FIG. 4. (a) Dependence of the averaged value of the noise power at 1 Hz normalized by the square of the current $\langle \mathcal{S}_v/I^2\rangle$ on the resistance of several different samples near the percolation threshold. □, irregular-particle–polymer composites; +, spherical-particle–polymer composites. The solid line is the fit obtained with relation (30) in the intermediary regime between type-1 and 2 contact behavior. The dashed lines represent $R^{\omega+2}$ with a slope $\omega=1.5$ at the low-resistance range and a slope $\omega=1.0$ at the high-resistance range, and calculated using the values $(R_1,\mathcal{S}_1)$ and $(R_2,\mathcal{S}_2)$ of Table I. (b) Dependence of the (commonly used) dimensionless noise power $\mathcal{S}_v=\langle \delta V^2/V^2\rangle$ at 1 Hz on the resistance of several different samples near the percolation threshold.

We have plotted the noise power $\mathcal{S}_v$ as a function of the resistance R, as the "good" representative quantities rather than as a function of the particle concentration. The reason for this is the following. Near the percolation threshold the electrical conduction is very inhomogeneous. This leads, in particular, to large fluctuations from sample to sample, due mainly to critical fluctuations. Therefore, if possible at all, determining an average dependence of the noise power or resistance on the copper concentration would require a prohibitively large number of samples.

V. INTERPRETATION AND DISCUSSION OF THE EXPERIMENTAL RESULTS

From the normalized noise-versus-resistance data of Fig. 4(a) we can clearly infer the presence of two conduction mechanisms: From a linear regression to the experimental data for the low-resistance values ($R < 10^4\ \Omega$) we get the value of $\omega=1.5\pm0.2$, and for the high-resistance linear region ($R > 10^7\ \Omega$) we obtain $\omega=1.0\pm0.3$. We interpret these data as follows. We assume that conduction in these copper-polymer composites is mainly dominated by two types of electrical contacts. The first type of contact (type 1), which essentially determines the conduction mechanism for the samples with low resistance, is of the metal-metal junction type, in the Sharvin limit (see Ref. 28). The second type of contact (type 2), dominating the high-resistance samples, is of a different nature, with higher resistance $r_2 \gg r_1$, and higher noise power, $\mathcal{S}_2 \gg \mathcal{S}_1$.

All data were taken in a very limited concentration interval close to the percolation threshold, where the conductive particles form a close-packed monolayer. The percolation transition is therefore associated with a change from one type of dominant contact to another. In the transition range there will be a random distribution of the two types of contacts with a probability distribution that depends on the details of sample-preparation procedure (cleaning, mixing, etc.; cf. Ref. 28). It is therefore reasonable to represent our system by a two-dimensional network with a fixed number of nodes and links. Each link will contain one contact of type 1 or 2 with, respectively, a probability p_1 or p_2, where $p_1+p_2=1$.

This brings about a difference between this model and the analysis presented by Mantese, Webb, and Curtin discussed in the Introduction.[24,25] In their case, the noise of cermets was studied in the whole domain of volume concentration of the conducting phases, and p_1 and p_2 are thus functions of the concentration. As a first approach we will develop a two-component effective-medium theory. For this purpose, we will make a further approximation by assuming an homogeneous lattice with resistors either r_1 or r_2. In this case, the probability distribution can be written as

$$p(g_i,\mathcal{S}_i)=p_1\delta(g_i-g_1)\delta(\mathcal{S}_i-\mathcal{S}_1)+p_2\delta(g_i-g_2)\delta(\mathcal{S}_i-\mathcal{S}_2)\,. \quad (28)$$

In this model the values $(R_1,\mathcal{S}_1)$ and $(R_2,\mathcal{S}_2)$ represent the resistance and the total noise power for a perfect lat-

TABLE I. Values used in the disordered resistor-lattice model.

R_1 (Ω)	R_2 (Ω)	$\mathcal{S}_1$	$\mathcal{S}_2$
6.4×10^1	2.3×10^8	1.8×10^{-9}	1.1×10^{-5}

tice where there are only resistors of type 1 (or type 2).

After elimination of p_1 and p_2 from the effective-medium equations [Eqs. (15) and (16)], and using the probability distribution of Eq. (28), we can express the average noise power $\mathcal{S}_m$ for this lattice as a function of average total resistance R_m. For a square resistor network, where $z/2=2$, we get the simple result

$$\mathcal{S}_m=\frac{R_m}{R_1-R_2}\left[\frac{R_m^2(\mathcal{S}_1-\mathcal{S}_2)+(R_1^2\mathcal{S}_2-\mathcal{S}_1R_2^2)}{R_m^2+R_1R_2}\right] . \quad (29)$$

In particular, if the inequalities $R_1 \ll R_2$ and $\mathcal{S}_1 \ll \mathcal{S}_2$ hold, then Eq. (29) reduces to

$$\mathcal{S}_m=\frac{R_m}{R_2}\left[\frac{R_m^2\mathcal{S}_2+R_2^2\mathcal{S}_1}{R_m^2+R_1R_2}\right] . \quad (30)$$

Figure 4(a) shows the fit of Eq. (30) to the experimental data. The values of $(R_1,\mathcal{S}_1)$ and $(R_2,\mathcal{S}_2)$ are given in Table I.

By solving the integrals of Eqs. (15) and (16) for this system, and using the values for R_i and $\mathcal{S}_i$ from Table I, we can relate p_1 and p_2 to the total resistance R_m and total noise $\mathcal{S}_m$. The result is plotted in Fig. 5. The two curves take the characteristic form of a two-component effective-medium theory.

For values of p_2 where $(R_1,\mathcal{S}_1)$ are dominant [and similarly for $(R_2,\mathcal{S}_2)$], we have a behavior similar to the one-component effective-medium theory. Let us note that in this case, when introducing the local relation $(\mathcal{S}_r \sim r^{\omega})$, we automatically get the same functional dependence for the total average noise power versus total resistance $(\mathcal{S}_R \sim R^{\omega})$.

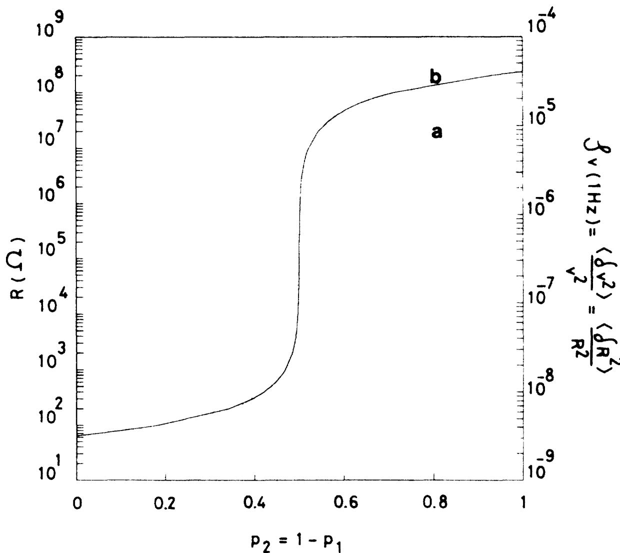

FIG. 5. Model calculation of the dependence of (a) the noise power S_v and (b) resistance R near the percolation transition on the theoretical probability $p_2=1-p_1$ to find a contact of type 2.

This allows us to identify the microscopic mechanism responsible for the noise power and the electrical contact resistance in these composites: for low resistance we measure $\mathcal{S}_R \sim R^{1.5}$, which corresponds exactly to the dependence expected for Sharvin-type metallic junctions [Eq. (8)]. In the second region, with the high-resistance values, we obtained $\mathcal{S}_R = R^{1.0}$, which is what we expect for a noisy contact limited by intrinsic conduction through a dirty oxide layer, as shown in Eq. (10).

R_1 and R_2 represent the values of the resistance of the perfect network ($p_c=0$ or 1). The ratio of those two values must be equal to the ratio of the microscopic resistances r_1 and r_2 in this two-component model. From Table I we get

$$R_2/R_1=3.6\times10^6=r_2/r_1 . \quad (31)$$

If we now take the ratio of the Sharvin contact resistance [Eq. (7)] and the oxide-limited weakly conducting barrier [Eq. (11)], we obtain

$$\frac{r_2}{r_1}=\frac{r_{\text{film}}}{r_{\text{Sharvin}}}=\frac{3}{4\pi^2}\frac{t\rho_{\text{ox}}}{\rho l} . \quad (32)$$

The quantity ρl is temperature independent—its value for copper is 6.6×10^{-16} Ω m^2. If we take an oxide-film thickness of 2 nm, we obtain from the previous expression an oxide resistivity $\rho_{\text{ox}}=20$ Ω m. This value is in good agreement with the measured value of resistivity for Cu_2O between 10 and 50 Ω m.[37] The curves in Fig. 6 allow the comparison of the temperature dependence for the two regimes with different types of contacts. These curves are only suggestive, as the differential expansion coefficients of the copper and the polymer induce some instability in the contacts and the resistance may vary in steps, particularly in the transition region where the current pattern becomes more and more filamentary. These curves show, however, that the temperature coefficient of the resistance is much weaker in the Sharvin-type contact than in the high-resistance regime, where semiconducting (Cu_2O) contacts dominate. We also present in the inset of Fig. 6 the behavior of the more resistive sample in a "classical" activation plot ($\log_{10}R$ versus T^{-1}). At high temperatures we observe almost linear dependence which is typical of a thermally activated process. It is well known that, at room temperature, defects account for the conduction mechanism in Cu_2O, and an excess of oxygen gives p-type conduction.[18,38,39]

We cannot exclude the possibility of other types of junctions and, thus, of yet another conduction mechanism, as these could also give other dependences on temperature, such as, for instance, tunneling between small particles, which, in some cases, can give a strong T dependence and which could be present in samples at the very high resistance values.

However, as other arguments supporting our interpretation of the noise as being due to an intrinsic semiconducting barrier, we would like to mention the high value of the percolation threshold and also the influence of the electric field, the frequency dependence, and the non-

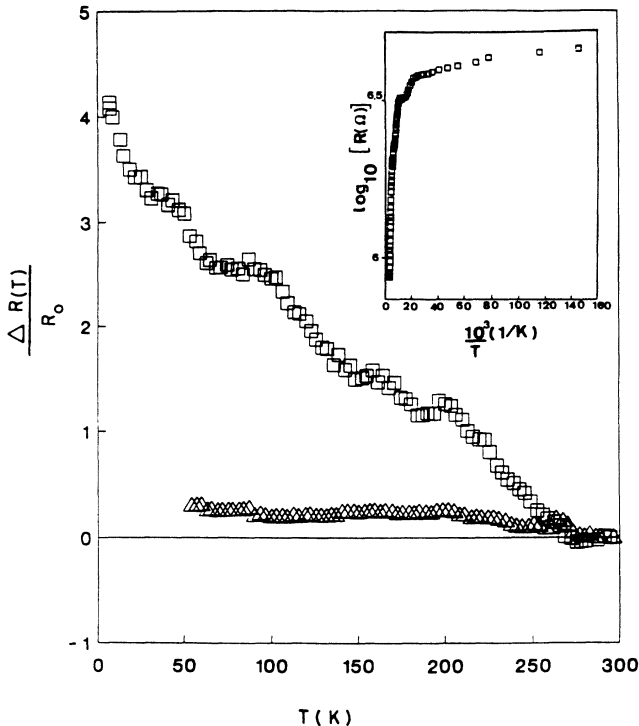

FIG. 6. Temperature dependence of the resistance for two samples in the two different regimes of contact. The lower curve (△), for a sample with $R=2.7\times10^3$ Ω, shows a much weaker variation than the upper curve (□), for a sample with $R=9.3\times10^5$ Ω. The inset shows—for the more resistive sample of $R=9.3\times10^5$ Ω—$\log_{10}[R(\Omega)]$ vs $1/T$, to reveal the activated character of the resistance.

linearities at high currents in the sample. In the "critical" region around 10^6 Ω, when R increases further, the one type junction (Sharvin) is replaced by the other type of junction (oxide). The decrease of dominance of the type-1 junctions is responsible for an increase of the total noise. The number of type-2 junctions is also reduced and the major part of the external voltage is found across the intergranular dirty contacts. This explains the extreme sensitivity to high electric fields of samples with a resistance near this critical value. However, for more resistive samples most of the current contacts are oxidized. The potential distribution on the whole lattice is more homogeneous and the total voltage necessary to induce electrical breakdown in the oxide is higher. The $f^{-\gamma}$ frequency dependence of the noise, with γ different from 1, could also be related to the distribution of the potential differences applied to the oxide junctions, which could create a time dependence of the contact resistances, and this extra resistance variation can give rise to an apparent $1/f$ noise.[8]

A last point we want to discuss is relative to the current pattern near the percolation threshold.

In order to check the homogeneous or inhomogeneous character of the conduction, we have used the following original method. As any resistive contact gives away some heat, we have tried to map the conducting filaments by infrared thermography. Infrared pictures of the surface, taken with a liquid-nitrogen-cooled far-infrared ($\lambda=8-10$ μm) prototype camera (SABCA, Brussels), with 1 μm resolution, were taken for samples with different resistances, and an example is shown in Fig. 7.

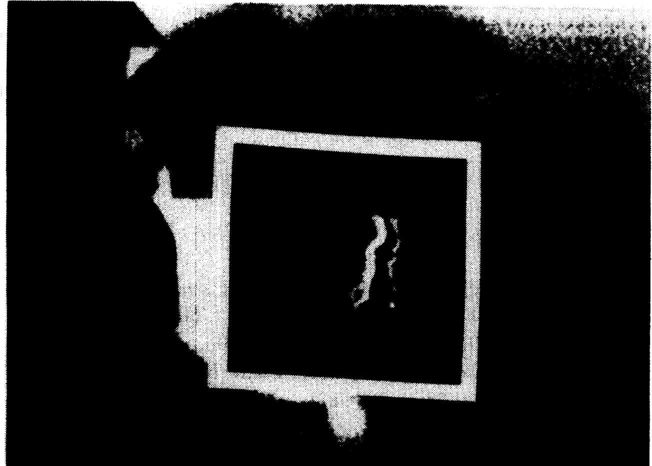

FIG. 7. Direct observation of the filamentary conducting path in the percolation transition, using far-infrared thermography. The white frame represents the limit of the sample; the side length is 5 cm.

The thermographs clearly show filamentary conduction paths in these samples. One should note, however, that in order to get such pictures it was necessary to drive rather larger currents (≈ 100 mA) through the sample for sufficient heat production. At those values of current and, consequently, of voltage applied to the junctions, some melting of the conducting paths occur, as we discussed above.

We think, however, that these pictures illustrate the inhomogeneous character of conduction close to the percolation threshold. The basic reason for such a behavior is the critical fluctuation regime, which dominates at $p \sim p_c$. The length scale which describes this limit is the diverging correlation length (ξ).[40–43]

VI. CONCLUSIONS

In this work we have made a comprehensive study of the electrical $1/f$ noise in polymer–copper-particle composite materials close to the percolation threshold. We have shown that it is possible to relate the global noise-power–resistance dependence in the percolation limit to the local noise produced by the microcontacts separating the particles in the composites.

We have presented an extension of the well-known effective-medium theory, and have shown experimentally that the node-link-node model gives a good description of the conducting backbone preexisting in real physical systems near the percolation transition. The microbridge model introduced is in agreement with that given in the preceding paper[28] for the high-particle-concentration limit and gives a new example of a percolation scheme in physical systems.

ACKNOWLEDGMENTS

We would like to thank Professor J. Jeener and Professor M. Mehbod for valuable discussions and suggestions. This work was supported by the Institut pour la Recherche Scientifique dans l'Industrie et l'Agriculture (for C. P.), the European Economic Communities under Contract No. ST280, and the Communauté Française de Belgique.

[1]N. M. Zimmerman and W. W. Webb, Phys. Rev. Lett. **61**, 889 (1988).

[2]G. A. Garfunkel, G. B. Alers, M. B. Weissman, J. M. Mochel, and D. J. Vanharlingen, Phys. Rev. Lett. **60**, 2773 (1988).

[3]S. Hershfield, Phys. Rev. B **37**, 8557 (1988).

[4]J. H. Scofield and J. V. Mantese, Phys. Rev. B **32**, 736 (1985); Phys. Rev. Lett. **54**, 353 (1985).

[5]J. Pelz and J. Clarke, Phys. Rev. B **36**, 4479 (1987).

[6]F. N. Hooge, T. G. M. Kleinpenning, and L. K. J. Vandamme, Rep. Prog. Phys. **44**, 480 (1981).

[7]A. van der Ziel, Adv. Electron. Electron Phys. **49**, 225 (1979).

[8]P. Dutta and P. M. Horn, Rev. Mod. Phys. **53**, 497 (1981).

[9]M. B. Weissman, Rev. Mod. Phys. **60**, 537 (1988).

[10]R. Rammal, C. Tannous, and A.-M. S. Tremblay, Phys. Rev. A **31**, 2662 (1985).

[11]R. Rammal, C. Tannous, P. Breton, and A.-M. S. Tremblay, Phys. Rev. Lett. **54**, 1718 (1985).

[12]R. Rammal, in *Fractals in Physics,* edited by L. Pietonero and E. Tosatti (Elsevier, Amsterdam, 1986), p. 373; R. Rammal and A.-M. S. Tremblay, Phys. Rev. Lett. **58**, 415 (1987).

[13]W. T. Elam, A. R. Kerstein, and J. J. Rehr, Phys. Rev. Lett. **52**, 1516 (1984).

[14]I. Halperin, S. Feng, and P. N. Sen, Phys. Rev. Lett. **54**, 2391 (1985).

[15]A.-M. S. Tremblay, S. Feng, and P. Breton, Phys. Rev. B **33**, 2077 (1986).

[16]S. Feng, B. I. Halperin, and P. N. Sen, Phys. Rev. B **35**, 197 (1987).

[17]I. Balberg, N. Wagner, D. W. Hearn, and J. A. Ventura, Phys. Rev. Lett. **60**, 1887 (1988).

[18]R. Holm, *Electric Contacts Handbook,* 3rd ed. (Springer-Verlag, Berlin, 1958).

[19]J. L. Williams and R. K. Burdett, J. Phys. C **2**, 298 (1969).

[20]M. Celasco, A. Masoero, P. Mazzetti, and A. Stepanescu, Phys. Rev. B **17**, 2553 (1978); **17**, 2564 (1978).

[21]C. C. Chen and Y. C. Chou, Phys. Rev. Lett. **54**, 2529 (1985).

[22]G. A. Garfunkel and M. B. Weissman, Phys. Rev. Lett. **55**, 296 (1985).

[23]R. H. Koch, R. B. Laibowitz, E. I. Alessandrini, and J. M. Viggiano, Phys. Rev. B **32**, 6932 (1985).

[24]J. V. Mantese and W. W. Webb, Phys. Rev. Lett. **55**, 2212 (1985).

[25]J. V. Mantese, W. A. Curtin, and W. W. Webb, Phys. Rev. B **33**, 7897 (1986).

[26]R. Rammal, J. Phys. (Paris) Lett. **46**, L129 (1985).

[27]M. Octavio, G. Guterierrez, and J. Aponte, Phys. Rev. B **36**, 2461 (1987).

[28]C. Pierre, R. Deltour, J. A. A. J. Perenboom, and P. J. M. Van Bentum, this issue, the preceding paper, Phys. Rev. B **42**, 3380 (1990).

[29]A. I. Akimenko, A. B. Verkin, and I. K. Yanson, J. Low Temp. Phys. **54**, 247 (1984).

[30]L. K. J. Vandamme, J. Appl. Phys. **45**, 4563 (1974).

[31]L. K. J. Vandamme and R. P. Tijburg, J. Appl. Phys. **47**, 2056 (1976).

[32]P. M. Kogut and J. P. Straley, J. Phys. C **12**, 2151 (1979).

[33]E. O. Brigham, *The Fast Fourier Transform* (Prentice-Hall, Englewood Cliffs, NJ, 1972).

[34]J. Max, *Traitement du Signal I* (Masson-Cie, Paris, 1972).

[35]*Metal-Filled Polymers,* edited by Swapan K. Bhattacharya (Dekker, New York, 1986).

[36]F. F. T. de Araujo and H. M. Rosenberg, J. Phys. D **9**, 1025 (1976).

[37]*Handbook of Chemical Physics,* 67th ed., edited by Robert C. Weast (Chemical Rubber Co., Boca Raton, FL, 1987).

[38]A. Haydar, A. Coret, and N. Oudjehane, Phys. Status Solidi **70**, 683 (1982).

[39]C. P. Massolo, M. Renteria, J. Desimoni, and A. G. Bibiloni, Phys. Rev. B **37**, 4743 (1988).

[40]*Electrical Transport and Optical Properties of Inhomogeneous Media (Ohio State University, 1977),* Proceedings of the First Conference on the Electrical Transport and Optical Properties of Inhomogeneous Media, AIP Conf. Proc. No. 40, edited by J. C. Garland and D. B. Tanner (AIP, New York, 1978).

[41]Percolation Structures and Processes, edited by G. Deutscher, R. Zallen, and J. Adler [Ann. Israel Phys. Soc. **5** (1983)].

[42]*Ill-Condensed Matter,* edited by R. Balian, R. Maynard, and G. Toulouse, Les Houches Session XXXI (North-Holland, Amsterdam, 1978).

[43]*Chance and Matter,* edited by J. Soulletie, J. Vannimanus, and R. Stora, Les Houches Session XLVI (North-Holland, Amsterdam, 1987).

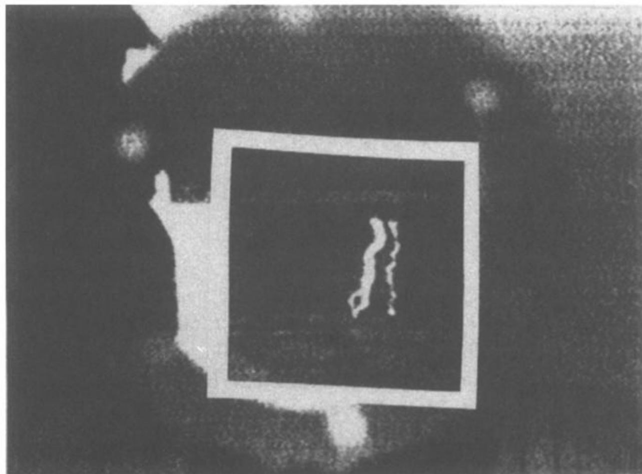

FIG. 7. Direct observation of the filamentary conducting path in the percolation transition, using far-infrared thermography. The white frame represents the limit of the sample; the side length is 5 cm.